

RED BLOOD CELL DEFORMABILITY UPON CONTINUOUS OR REPETITIVE LOADINGS

Hiroaki Ito¹, Ryo Murakami¹, Chia-Hung Dylan Tsai¹, Mitsuhiro Horade¹,
Motomu Tanaka², and Makoto Kaneko¹

¹Department of Mechanical Engineering, Osaka University, Osaka, JAPAN

²Institute of Physical Chemistry, University of Heidelberg, Heidelberg, GERMANY

ABSTRACT

This paper focuses on the comparison of red blood cell (RBC) deformability under continuous and repetitive loadings. We utilized a feedback position-control system and a narrow microfluidic channel for applying different deformation patterns on RBCs. According to the analyses of shape recoveries with different patterns, we found, for the first time, that the mechanical responses of RBCs upon continuous and repetitive loadings are almost the same within the error among cellular individualities as long as the total duration of the loading is the same. The result indicates that the internal mechanical stress on RBCs accumulates even if the apparent cell shape recovers. The finding provides quantitative insights for the systematic comparison among various existing measurement methods of mechanical responses of cells.

INTRODUCTION

Red blood cell (RBC) deformability in microvasculatures is an important property for smooth microcirculation. Toward better understanding and treatments of blood health conditions, microfluidic techniques for evaluating the deformability of rapidly flowing RBCs have been developed so far. In this context, representative responses upon the deformation inside the microchannel have been quantified through extensibility (aspect ratio of a stretched shape) and transit time, which are measured through visual images [1,2,3], pressure drop [4], and electrical impedance of the microchannel [5]. Because RBCs inside a microfluidic channel, typically made of polydimethylsiloxane (PDMS) bounded to a glass substrate, are accessible only via the inlet or outlet holes, limited stress pattern has been studied, for example, steady shear flow [2,6] or spatial constriction narrower than RBC diameter [1,3] under constant flow rate. However, it is critically important to systematically investigate the response characteristics of RBCs for various deformation patterns, as they experience in various kinds of blood microvessels with different shapes under different flow rates *in vivo*. As an extreme cases of deformation pattern *in vitro*, Sakuma *et al.* performed a repetitive fatigue assay, in which a mechanical stress from a narrow constriction is applied to a RBC as frequent as possible using ultra high speed on-chip manipulation [6]. After thousands of passages through the narrow constriction, RBCs lose their deformability. On the other hand, Murakami *et al.* performed “Catch-Load-Launch” manipulation to apply a single continuous loading to a RBC *in vitro* for a desired time

duration. Nevertheless, it still remains unclear how RBCs respond to different patterns of applied stress in principle, due to the lack of precisely spatiotemporal controlled experiments for RBCs inside a narrow microchannel.

This paper shows a precisely controlled measurement of viscoelastic responses of RBCs. Figure 1 shows an essential design of our experimental approach. By manipulating the cell position inside the microchannel, we reveal the effect of the number m of deformation at a narrower constriction. To fairly compare the difference between continuous ($m = 1$) and repetitive ($m \geq 2$) deformation, we set the two conditions with different number m (equivalent to loading frequency) but the same total loading duration. After these two different loadings, we launch the RBC and kept outside of the channel for the shape recovery. Finally, the shape recovery is evaluated through the cell height H as a function of recovery time t .

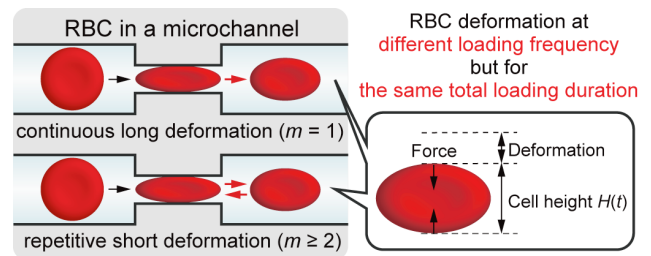


Figure 1: Red blood cell (RBC) deformation by passing through a narrow channel at different frequency but for the same duration. We evaluated the effect of the number m of passages ($m = 1$; continuous, $m \geq 2$; repetitive) on the shape relaxation after the constriction.

EXPERIMENTAL METHODS

Precise Manipulation for Controlled Deformation

To precisely apply the specified stress patterns on a RBC, we utilized a “robotic pump” system shown in Fig. 2, which enables to control the cell position inside a narrow microchannel at a spatial accuracy of $0.24 \mu\text{m}$ and at a control frequency of 1000 Hz [7,8]. “Robotic pump” is composed of a syringe, a piezo electric actuator (PST 150/5/40 VS10, Syouei System), and a high speed camera (IDP-Express R2000, Photron). The whole experimental system is shown in Figure 2. The syringe is connected to the outlet of a microfluidic channel via an Ethylen Tetrafluoroethylene (ETFE) tube and a silicone tube. The microchannel with $3.5 \mu\text{m} \times 10.0 \mu\text{m}$ (main channel) and

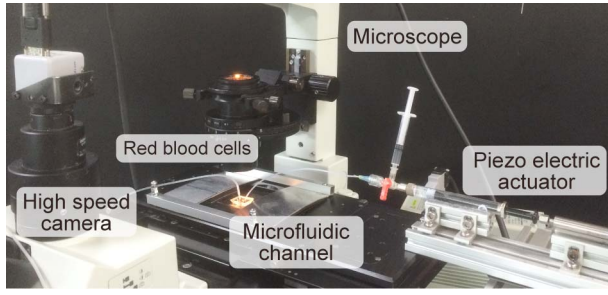


Figure 2: Overview of the experimental system. “Robotic pump” is composed of a syringe connected to a piezo electric actuator, which is driven based on a real time visual feedback information obtained from a high speed camera.

$3.5 \mu\text{m} \times 3.0 \mu\text{m}$ (narrow constriction) cross sections is made between a glass slide and PDMS (SILPOT 184, DOW CORNING TORAY). The microfluidic chip is mounted on a optical microscope (IX71, Olympus) equipped with a $\times 40$ objective lens (N.A. = 0.6) and a high speed camera. The optical image of a RBC is acquired and processed to extract the RBC position at 1000 Hz. Then, the position is converted to a voltage input for the piezo electric actuator, based on a proportional-integral-derivative (PID) algorithm, to control the pressure at the outlet of the channel. This real time feedback loop enables the ultra-high speed and ultra precise cell manipulation in a microchannel.

Human RBCs are freshly drawn from a healthy volunteer donors with informed consent, and dispersed in standard saline at a blood concentration of 1% (v/v). The dispersed RBCs are injected into the the microfluidic channel via the inlet using a ETFE and silicon tube. Under a constant pressure difference between the inlet and outlet, which is maintained by a gravitational force, the “robotic pump” additionally control a fine pressure at the outlet.

Deformation Pattern

Figure 3 shows fundamental deformation patterns characterized by two principal parameters, frequency ω and duty ratio d of loading for RBCs, in a certain time duration $2T$. The total duration of loading is determined by the multiplication of $2T$ and d regardless of the frequency ω . In our experiment, we set as $d = 0.5$ and $T = 100$ s, and thus the total loading time inside the narrow constriction was fixed to $2Td = 100$ s. Under this constant stress level, we investigated the effect of loading frequencies ω . We set $\omega = m/2T = 0.005$ Hz and 0.05 Hz, which correspond to $m = 1$ and 10 , respectively. Note that the information of frequency ω is equivalent to the number of passages m in the duration $2T$. Thus, $\omega = 0.005$ Hz is a continuous loading and $\omega = 0.05$ Hz is a ten times repetitive loadings.

RESULTS AND DISCUSSION

Precise Manipulation inside a Microchannel

Figure 4 shows a visual scheme of the cell manipulation that realizes the continuous and repetitive loadings in our experimental system. First, a flowing RBC is caught in front of the narrow constriction, and kept there for 2 s to restore the original biconcave RBC shape prior to the loading experiment. Then, in the loading phase, the RBC is moved into/out-of the constriction after being kept for each T/m s for $d = 0.5$. Finally, after m cycles, the RBC is launched and the shape recovery is recorded in sequential snapshots. Only for the first T/m s outside the narrow constriction, the RBC is kept at the inlet side, whereas the following T/m s outside it is kept at the outlet side. Figure 5 shows the results of the actual manipulation under the conditions of $m = 1$ (Figure 5a, red) and $m = 10$ (Figure 5b, blue). While the position of RBC stably follows to the target signal in a resting phase, it needs to some relaxation time to follow the step-like target

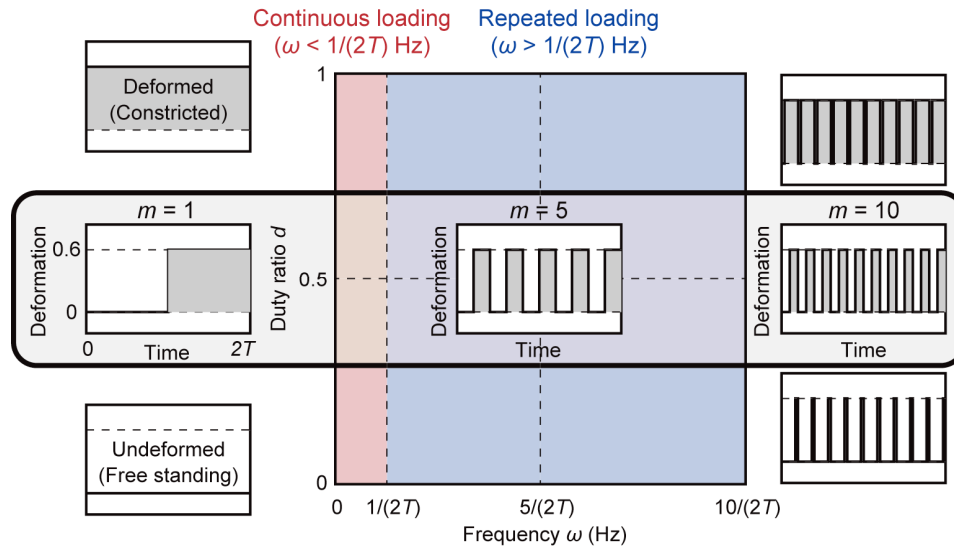


Figure 3: Schematic diagram of characteristic deformation pattern. Frequency ω and duty ratio d can be the representative parameters for RBC deformation. We set as $d = 0.5$ and $T = 100$ s with the fixed total loading time $2Td = 100$ s in this study. The number of deformation m was set as $m = 1$ and 10 , which corresponds to the frequency $\omega = m/2T = 0.005$ Hz and 0.05 Hz, respectively (left and right patterns shown in shaded area).

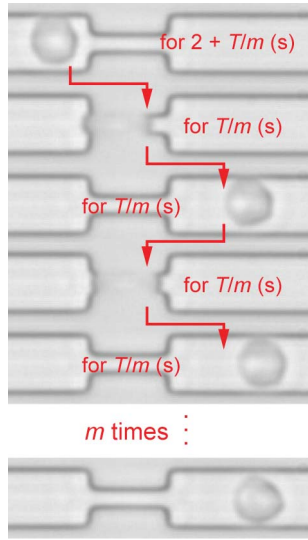


Figure 4: Examples of m times repetitive manipulation of a RBC around a narrow constriction.

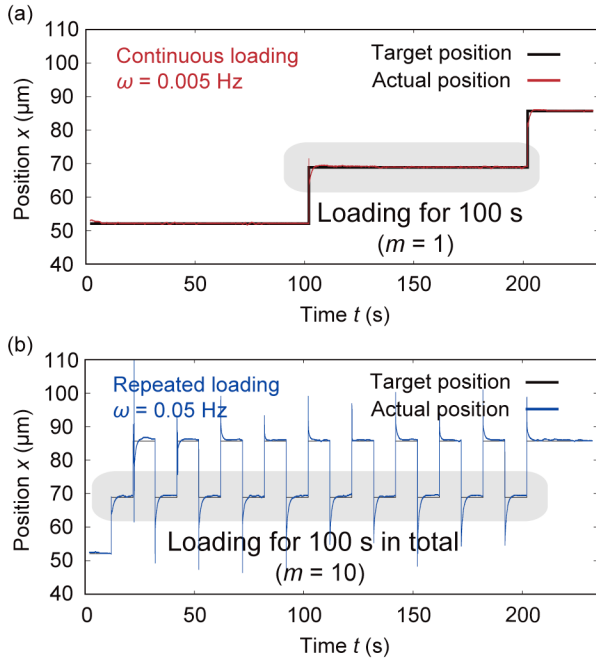


Figure 5: (Black) Target and (red/blue) actual cell positions x for (a) one continuous loading and (b) ten times repetitive loadings in the microchannel during the manipulation. Total manipulation time $2T = 200$ s and duty ratio $d = 0.5$.

motion (black) because the the sampling frequency of the target position 1000 Hz is so high. Such a delay after the step-like manipulation is seen especially in the second or later cycles, probably because of an integral term of PID control. Nevertheless, duration of the constricted deformation is well controlled as visualized by the shaded gray areas, which represent the cell position inside the narrow constriction, in Figure 5. As a result, we successfully applied well controlled loadings on RBCs at the specified parameters (T ; ω , d).

Shape Recovery

After the loadings, the shape recoveries were observed at the wider part for up to tens of seconds with the aid of the high-speed visualization at a 1000 Hz temporal resolution. Figure 6a shows the recorded optical images of cell shape recoveries in the cases of loading frequencies $\omega = 0.005$ Hz ($m = 1$, left) and $\omega = 0.05$ Hz ($m = 10$, right). In both cases, RBCs were launched from the narrow constriction in ~ 5 ms, and immediately recovered to a certain level of each original shape. This fast response is governed by an elastic features of RBCs. After that, the RBCs further recovered their shapes to the original biconcave shapes in a much slower manner. This slow recovery typically took 1-10 s, and is governed by a viscoelastic feature. Figure 6b shows the time course of the cell height H as a function of recorded time t . The amplitude was normalized by the original cell height $H(0)$ obtained in front of the narrow constriction prior to performing the loading experiment. The dashed red line and solid blue line corresponds to the mean values of $H(t)/H(0)$, which were calculated as the average of 5 cells for each loading frequency ω . The shaded area for each ω represents the standard deviation (S.D.). This result surprisingly indicates that the mechanical resthese of a RBC is independent of these two loading frequency conditions within the error among 5 cells for each.

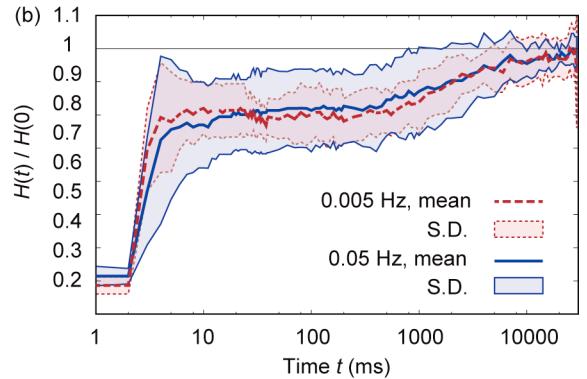
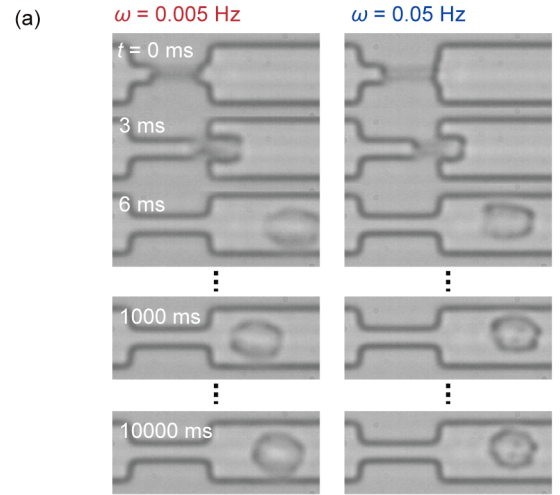


Figure 6: (a) Examples of shape recovery after launching. (b) Comparison between one and ten times loadings.

Evaluation of viscoelastic property

To evaluate the shape recovery more quantitatively, we compared the obtained mean recovery (Figure 6b, lines) to a theoretical viscoelastic model. Here we used an ideal viscoelastic model consisting of two linear elastic spring (spring constant k_1 and k_2) and two viscous dampers (damping coefficient c_1 and c_2). The viscous damper (c_1) is serially connected to the standard linear solid (SLS) model, which is the parallel combination of a spring (k_1) and the Maxwell model (k_2 and c_2). Using this “standard linear elastic” (SLE) model, we performed least square fittings for the two experimental curves. Because our experimental system does not include a force sensor, we can only evaluate a ratio of a damper and a spring, namely, characteristic times for them. In particular, characteristic recovery time τ of a whole model is represented as $\tau = c_2(k_1+k_2)/(k_1k_2)$. Here we evaluated the ratio with respect to k_1 , a spring constant of a separately parallelized spring in SLE model. Table 1 shows the calculated ratios of the parameters (k_2/k_1 , c_1/k_1 and c_2/k_1) and the characteristic recovery time τ for the two different frequencies $\omega = 0.005$ Hz ($m = 1$) and 0.05 Hz ($m = 10$). The fitting result quantitatively shows the same mechanical responses within the error from RBC individuality, which fills the gap between separated understandings of a continuous loading [8] and repetitive loadings [7]. For a possible physiological relevance, the result also indicates that the internal mechanical stress on RBCs accumulates even if the apparent cell shape recovers. Because the internal properties may include characteristic viscoelastic or plastic properties of cell membrane, cytoskeleton, and cytoplasm, to decompose the obtained viscoelastic parameters into these characteristics will also be an interesting future work for better understanding of RBC mechanics. Moreover, the mechanical responses characteristic for the RBC internal structure may also contribute to a novel diagnosis based on cell mechanics.

Table 1: Evaluated mechanical parameters from curve fittings with SLE model.

Loadings	Continuous	Repetitive
m	1	10
k_2/k_1	0.37 ± 0.21	0.36 ± 0.08
c_1/k_1 (s)	58.8 ± 2.0	58.1 ± 2.8
c_2/k_1 (s)	0.96 ± 0.73	0.74 ± 0.22
τ (s)	5.17 ± 4.61	2.85 ± 0.90

CONCLUSIONS

RBC deformability upon different loading patterns is investigated using a microfluidic constriction and on-chip precise manipulation by “robotic pump”. We kept the total deformation amplitude and duration time as constant, and performed loading test of RBCs under the two different frequencies by an order of magnitude. One is a long-lasting single loading, and the other is ten times repetitive loadings, which corresponds to 100 s deformation in total in the both cases. To evaluate the cell shape recoveries, we analyzed the normalized cell height. Through the comparison of the two

different frequencies and we found that the shape recovery is the same as long as the total deformation level is the same. Our demonstration and finding provide a quantitative criteria for quantitative comparisons between different loadings on RBCs. Further tuning of the PID gains for the present experimental setup will improve both the throughput and stability, leading to a novel on-chip evaluator of cell mechanics for any desired deformation patterns.

ACKNOWLEDGEMENTS

We thank Dr. S. Sakuma and Prof. F. Arai for supporting the experimental setups. This work was supported by JSPS KAKENHI JP16H06933 and JP13J01297 (H.I.), JP16K18051 (C.-H.D.T.), JP15H05761 (M.K.), and Sasakawa Scientific Research Grant from The Japan Science Society 28-233 (H. I.).

REFERENCES

- [1] S. S. Shevkoplyas, T. Yoshida, S. C. Gifford, M. W. Bitensky, “Direct measurement of the impact of impaired erythrocyte deformability on microvascular network perfusion in a microfluidic device”, *Lab Chip*, vol. 6, pp. 914-920, 2006.
- [2] G. Tomaiuolo, M. Barra, V. Preziosi, A. Cassinese, B. Rotoli, S. Guido, “Microfluidics analysis of red blood cell membrane viscoelasticity”, *Lab Chip*, vol. 11, pp. 449-454, 2011.
- [3] C.-H. D. Tsai, J. Tanaka, M. Kaneko, M. Horade, H. Ito, T. Taniguchi, T. Ohtani, Y. Sakata, “An on-chip RBC deformability checker significantly improves velocity-deformation correlation”, *Micromachines*, vol. 7, pp. 176:1-13, 2016.
- [4] M. Abkarian, M. Faivre, R. Horton, K. Smistrup, C. A. Best-Popescu, H. A. Stone, “Cellular-scale hydrodynamics”, *Biomedical Materials*, vol. 3, pp. 034011:1-13, 2008.
- [5] Y. Zheng, E. Shojaei-Baghini, A. Azad, C. Wang, Y. Sun, “High-throughput biophysical measurement of human red blood cells”, *Lab Chip*, vol. 12, pp. 2560-2567, 2012.
- [6] O. Otto, *et al.*, “Real-time deformability cytometry: on-the-fly cell mechanical phenotyping”, *Nat. Methods*, vol. 12, pp. 199-202, 2015.
- [7] S. Sakuma, K. Kuroda, C.-H. D. Tsai, W. Fukui, F. Arai, M. Kaneko, “Red blood cell fatigue evaluation based on the close-encountering point between extensibility and recoverability”, *Lab Chip*, vol. 14, pp. 1135-1141, 2014.
- [8] R. Murakami, C.-H. D. Tsai, H. Ito, M. Tanaka, S. Sakuma, F. Arai, M. Kaneko, “Catch, Load and Launch toward On-Chip Active Cell Evaluation”, *2016 IEEE International Conference on Robotics and Automation (ICRA2016, Stockholm, Sweden)*, pp. 1713-1718, 2016.

CONTACT

*H. Ito, tel: +81-6-6879-7333;
ito@hh.mech.eng.osaka-u.ac.jp